

V. Parail, R. Albanese, R. Ambrosino, J-F. Artaud, K. Besseghir, M. Cavinato,  
G. Corrigan, J. Garcia, L. Garzotti, Y. Gribov, F. Imbeaux, F. Koechl,  
C.V. Labate, J.B. Lister, X. Litaudon, A. Loarte, P. Maget, M. Mattei,  
D. McDonald, E. Nardon, G. Saibene, R. Sartori, J. Urban  
and JET EFDA contributors

# Self-Consistent Simulation of Plasma Scenarios for ITER Using a Combination of 1.5D Transport Codes and Free Boundary Equilibrium Codes



# Self-Consistent Simulation of Plasma Scenarios for ITER Using a Combination of 1.5D Transport Codes and Free Boundary Equilibrium Codes

V. Parail<sup>1</sup>, R. Albanese<sup>2a</sup>, R. Ambrosino<sup>2b</sup>, J-F. Artaud<sup>3</sup>, K. Besseghir<sup>4</sup>, M. Cavinato<sup>5</sup>, G. Corrigan<sup>1</sup>, J. Garcia<sup>3</sup>, L. Garzotti<sup>1</sup>, Y. Gribov<sup>6</sup>, F. Imbeaux<sup>3</sup>, F. Koechl<sup>7</sup>, C.V. Labate<sup>2</sup>, J.B. Lister<sup>4</sup>, X. Litaudon<sup>3</sup>, A. Loarte<sup>6</sup>, P. Maget<sup>3</sup>, M. Mattei<sup>2c</sup>, D. McDonald<sup>1</sup>, E. Nardon<sup>3</sup>, G. Saibene<sup>5</sup>, R. Sartori<sup>5</sup>, J. Urban<sup>3</sup> and JET EFDA contributors\*

*JET-EFDA, Culham Science Centre, OX14 3DB, Abingdon, UK*

<sup>1</sup>*EURATOM-CCFE Fusion Association, Culham Science Centre, OX14 3DB, Abingdon, OXON, UK*

<sup>2a</sup>*Association EURATOM-ENEA-CREATE and University of Naples "Federico II", Italy*

<sup>2b</sup>*Association EURATOM-ENEA-CREATE and University of Naples "Parthenope", Italy*

<sup>2c</sup>*Association EURATOM-ENEA-CREATE and Second University of Naples, Italy*

<sup>3</sup>*CEA, IRFM, F-13108 St Paul-Lez-Durance, France*

<sup>4</sup>*Association EURATOM-Confédération Suisse, CRPP-EFPL, 1015 Lausanne, Switzerland*

<sup>5</sup>*Fusion for Energy, Barcelona, Spain*

<sup>6</sup>*ITER Organization, Route de Vinon sur Verdon, 13115 St Paul Lez Durance, France*

<sup>7</sup>*Association EURATOM-ÖAW/ATI, Atominstitut, TU Wien, 1020 Vienna, Austria*

\* See annex of F. Romanelli et al, "Overview of JET Results",  
(24th IAEA Fusion Energy Conference, San Diego, USA (2012)).

Preprint of Paper to be submitted for publication in Proceedings of the  
24th IAEA Fusion Energy Conference (FEC2012), San Diego, USA

8th October 2012 - 13th October 2012

“This document is intended for publication in the open literature. It is made available on the understanding that it may not be further circulated and extracts or references may not be published prior to publication of the original when applicable, or without the consent of the Publications Officer, EFDA, Culham Science Centre, Abingdon, Oxon, OX14 3DB, UK.”

“Enquiries about Copyright and reproduction should be addressed to the Publications Officer, EFDA, Culham Science Centre, Abingdon, Oxon, OX14 3DB, UK.”

The contents of this preprint and all other JET EFDA Preprints and Conference Papers are available to view online free at [www.iop.org/Jet](http://www.iop.org/Jet). This site has full search facilities and e-mail alert options. The diagrams contained within the PDFs on this site are hyperlinked from the year 1996 onwards.

## **ABSTRACT**

This paper discusses results of predictive modelling of all reference ITER scenarios and variants using two suites of linked transport and equilibrium codes. The first suite consisting of the 1.5D core/2D SOL code JINTRAC [1] and the free boundary equilibrium evolution code CREATE-NL [2], was mainly used to simulate the inductive D-T reference Scenario-2 with fusion gain  $Q = 10$  and its variants in H, D and He (including ITER scenarios with reduced current and toroidal field). The second suite of codes was used mainly for the modelling of Hybrid and Steady State ITER scenarios. It combines the 1.5D core transport code CRONOS [3] and the free boundary equilibrium evolution code DINA-CH [4].

## **1. INTRODUCTION**

Self-consistent predictive simulation of ITER scenarios is a very important tool for the exploration of the operational space and for scenario optimisation. It also provides an assessment of the compatibility of the developed scenarios (including fast transient events) with machine constraints. Credible prediction of the plasma and plasma-control systems behaviour can only be achieved when the best high quality 1.5D core transport codes are combined with state of the art free boundary equilibrium evolution codes. This paper discusses results of predictive modelling of all reference ITER scenarios and variants using two suite of linked transport and equilibrium codes. The first suite comprises the 1.5D transport code JINTRAC [1] and the free boundary equilibrium evolution code CREATE-NL [2] was mainly used to simulate the inductive burn 15MA Scenario with fusion gain  $Q = 10$  and its variants in H, D and He. The second suite combines 1.5D core transport code CRONOS [3] and the free boundary equilibrium evolution code DINA-CH [4] and was used for the modelling of hybrid and steady state scenarios.

The paper is organised as follows. Chapter 2 is devoted to a detailed description of the reference 15MA inductive burn scenario and its variants, assumptions and main modelling results. Chapter 3 describes Hybrid and Steady State (SS) scenarios as well as the main results of the modelling of these scenarios. Finally, Chapter 4 briefly summarises general results and discusses remaining issues.

## **2 15MA BASELINE INDUCTIVE BURN SCENARIO AND IT VARIANTS.**

### ***2.1 SPECIFICATION, MAIN ASSUMPTIONS AND MODELS.***

The characteristics of the 15MA inductive burn scenario with  $Q_{\text{fus}} = 10$  are summarised in tables 1-2 and we will refer to it as to Case#001. During the ramp-up phase, an early transition from the limited to the diverted phase is assumed, applying auxiliary heating right afterwards to reduce resistive flux losses.

When a current maximum of 15MA is reached, the auxiliary heating is increased to a maximum level to assure transition to type-I ELMy H-mode regime. As soon as the plasma density has reached a target level and the fusion process has fully developed, the auxiliary heating is reduced to reach

the maximum fusion gain  $Q_{\text{fus}} \approx 10$ . The flat-top phase is maintained until the CS coil flux charge limit for a safe H-L transition and plasma ramp-down is reached. The current and plasma density are then ramped down and auxiliary heating is gradually decreased. The H-L transition is assumed to occur at the beginning of ramp-down when the plasma energy content is still at its maximum level. This is the most difficult scenario for plasma control and allows testing if suitable plasma shapes and vertical stability can be maintained by the PF coil system under extreme conditions. The transition between the diverted and limited plasma at current ramp-down takes place at a low current level. The plasma discharge is simulated until plasma current drops below  $I_p < 1\text{MA}$ .

The Case#002 scenario only differs from Case#001 in its slower current ramp-down. This could be beneficial for fuelling, as the density limit  $n_{\text{GW}}$  scales with  $I_{\text{pl}}$  and it is not sure if the plasma particle content can be depleted quickly enough at high  $|dI_{\text{pl}}/dt|$  to stay below  $n_{\text{GW}}$ .

The Case#003 scenario is characterised by very short current ramp-up and ramp-down phases at maximum ramp rates that are achievable without violating PF coil power supplies voltage limits. The corresponding ramp-up/-down duration was found to be  $\approx 50\text{--}60\text{s}$ .

The Cases#1–3 assume that transition from limiter to divertor configuration during current ramp happens at  $I_{\text{pl}} \approx 4\text{MA}$ . To examine the sensitivity of plasma properties on the level of  $I_{\text{pl}}$  at the transition, another variant Case#004 with transition to/from diverted phase at  $I_{\text{pl}} \approx 7\text{MA}$  has been developed. Again, special attention was paid to the flux consumption balance. In the limiter phase, the heat flux crossing the separatrix is limited to avoid damage to the first wall.

Simulations have been also performed for the ITER pre-activation phase. The following three scenarios have been modelled:

- Case#005: H plasma,  $I_{\text{pl}} = 15\text{MA}$  at flat-top,  $B_0 = 5.3\text{T}$ .
- Case#006: H plasma,  $I_{\text{pl}} = 7.5\text{MA}$  at flat-top,  $B_0 = 2.65\text{T}$ .
- Case#007: He plasma,  $I_{\text{pl}} = 7.5\text{MA}$  at flat-top,  $B_0 = 2.65\text{T}$ .

Based on simulations for the 15MA ELMy H-mode ITER baseline scenario (Case#001) and sensitivity studies that have been made to find potentials of optimisation with respect to fusion energy production per discharge  $W_{\text{fus}}$ , new scenarios (Cases#007-010) have been developed where all beneficial factors have been combined.

Predictive modelling of the reference 15MA inductive burn scenario and its variants was also supplemented by an extensive analysis and modelling of fast transient phenomena, which include L-H and H-L transitions, strong ELMs and minor disruption. This study allowed us to test the ability of presently foreseen ITER position and vertical stability control system to cope with fast variation in total stored energy and plasma inductance.

CREATE-NL/JINTRAC coupling can be used in a strong or weak form. In the “strong” form, coupling is made time step by time step. This requires high computational times and can be reasonably run for a limited number of time steps, i.e. short time windows with a time step of 1–2ms (including eddy currents and VS controller simulation). The need to simulate voltsecond (VS) consumption on

significant time windows, forced us to also develop the “weak” coupling. In particular JINTRAC has been run using properly designed sequence of shapes and plasma currents. Then a free boundary simulation has been re-run with CREATE-NL using kinetic profiles from JINTRAC. The procedure was closed verifying that JINTRAC results are insensitive enough to shape variations simulated with the closed loop CREATE-NL runs. In JINTRAC, the evolution of core plasma is simulated in a semi-predictive way, with transport equations being always solved for current diffusion and heat transport but density being either prescribed or simulated. The Bohm/gyroBohm model is used in L-mode [5]. This choice is motivated by extensive model validation and benchmarking efforts that have been carried out during the past few years (see e.g. [6-7]). The GLF23 model [8] was selected for H-mode. Transition to H-mode is triggered when the total net plasma heating exceeds L-H transition power threshold from Martin et al. [9]. The GLF23 transport is assumed to be almost fully suppressed within edge transport barrier (ETB) after L-H transition. The ETB width was fixed in line with EPED model [10]. An empirical model is used to describe ELM-induced transport, which keeps plasma edge close to MHD stability limit inferred from MHD stability analysis. Heat deposition profiles were either calculated internally by JINTRAC models or prescribed following recommendations from ITER IO. Sawtooth reconnection is modelled by application of the Kadomtsev model. Flux consumption is determined following the axial representation described in [11].

One of the novel elements of this modelling was simulation of fast transient phenomena, such as L-H and H-L transition. Whereas the transition from H-mode to L-mode is prescribed in Cases#001-010, a self-consistent L-H transition model is used in supplementary studies. Depending on the assumptions, the behaviour of the transition can change featuring slow or fast change in energy content and some dithering between different confinement states.

All the free boundary simulations were produced with the CREATE-NL code [2]. This is an axisymmetric evolutionary free boundary equilibrium. It implements a first order FEM based on a Newton method for the solution of the free boundary nonlinear associated problem. A numerical calculation of the Jacobian matrices is adopted. CREATE-NL can account for the presence of eddy currents and iron. The feedback control action used in this study is composed of three parts:

- a vertical stabilization control of the plasma vertical position or speed using the VS3 circuit voltage;
- a control of the currents in the active coils using voltage in power supplies;
- a gap based shape control using reference currents to the lower level current control.

The controllers have been designed and used under the hypothesis that a feed-forward action in current is designed a-priori.

## **2.2. THE MAIN MODELLING RESULTS.**

*Optimisation of the plasma current ramp-up and ramp down:* A sensitivity scan for the ramp-up phase was performed with respect to  $dI_{pl}/dt$ , the amount of auxiliary heating, the density level and

boundary conditions (see Figure 1). If the current is ramped up at the maximum rate, the flat-top performance is degraded compared to the reference scenario (see Figure 2).). This degradation is caused by the decrease of the ratio  $s/q$  between shear and safety factor in the early phase of flat-top, causing an increase in the core micro turbulences according to experimental observations [12] and predictions with GLF-23 [13,14]. In the current ramp-down, the application of the maximum available current ramp rate helps to improve the Vs balance, but plasma control related to vertical stability and density pump-out becomes more demanding (see Figure 3 and [15]). Resistive flux losses are dominant in the late phase of ramp-down due to the decrease in temperature. With a late divertor-limiter phase transition, high  $P_{AUX}$  can be maintained at lower  $I_{pl}$  which helps to shape the current profile and reduce resistive losses.

*Sensitivity to timing of the L-H transition:*

Early transition to H-mode during current ramp-up helps to reduce Vs consumption [16]. However early L-H transition leads to a temporary reduction in plasma performance during initial phase of current flat top. Sensitivity to timing of the H-L transition: In order to reduce resistive and sawtooth-induced Vs losses, it is highly preferable to maintain H-mode conditions during ramp-down for as long as possible. The current ramp-down period could then be considerably enhanced. Simulations confirm that it should be possible to delay the H-L transition until  $I_p > 7MA$ .

*Self-consistent simulations of the plasma evolution after the L-H / H-L transition and sensitivity to H-L transition dynamic:*

One of the critical points observed when simulating 15MA Scenarios (Case#001 or Case#003) was the H to L transition. A scan in the foreseeable thermal energy decrease rate  $dW_{th}/dt$  after the H-L transition, depending on possible transitional plasma confinement states, was carried out and the extreme cases with the maximum conceivable  $dW_{th}/dt$  have been identified. Seven cases have been selected for further analysis with CREATE-NL. First, two reference cases: the attenuated H-L transition in Case#001 (henceforward referred to as case HL#1) and the fastest H-L transition (HL#2) at the end of the flat-top baseline scenario, were selected. Secondly, these two cases have been rerun with H-L transition shifted to an earlier stage of the flat-top phase where the transformer is far from the available flux limit (HL#3 resp. HL#4). Finally, three additional H-L transition cases with an attenuated (HL#5) and a sharp (HL#6) drop in energy and another case with intermittent transitions (HL#7) have been calculated using a self-consistent H-L transition model (see Figure 4). CREATE-NL simulations show that the change and the rate of change in  $\beta_{pol}$  are in a range where plasma shape control can become a challenge. The plasma column quickly approaches the inner wall after the transition, requiring a strong action from the central solenoid to decelerate its radial inward movement for the prevention of its contact with the inner wall. If an acceleration is given to the outward driving force though, one might risk to have poor shape control performance which may result in a contact with the outer wall just a few seconds later. The following degrees of

freedom on the control law that can have an impact on its efficiency and effectiveness were assumed in CREATE-NL controllability analysis:

- time update of the current nominal feed-forward control action (1s, 5s, mixed strategies),
  - possible delays in applying the feed-forward control action (may occur if the transition happens before the expected time),
- anticipation of the feedforward control action in time (as a possible strategy to avoid plasma-wall contact),
- scheduling of the feedforward control action with an on-line beta-poloidal estimate.

All the proposed sensitivity studies are related to finding the balance between feed forward and feedback actions. As for the feed forward current update sampling period we consider  $\tau_{ff} = 1s$  as the shortest period. The best strategy for the feed forward update is to have a 1s update just after the transition starts, and then have a 9 seconds update to avoid excessive movement of the plasma towards the external wall (see Figure 5). We conclude that plasma avoids wall contact even in the most dangerous, fastest transitions, although the minimum distance between separatrix and the inner wall temporarily drops below the safe distance. Optimisation of baseline inductive burn scenario. Based on simulations for the 15MA ITER inductive burn scenario and sensitivity studies, new scenarios have been developed where actions of all actuators were combined to maximise energy production per discharge  $W_{fus}$ . Three optimised scenarios S1-S3 have been tested and compared to Case #001:

- Scenario S1:  $I_{pl} = 15MA$  at flat-top,  $V_{loop} = 0.0V$  for  $I_{pl} = 15 \rightarrow 5MA$  at ramp-down
- Scenario S2:  $I_{pl} = 17MA$  at flat-top,  $V_{loop} = 0.0V$  for  $I_{pl} = 17 \rightarrow 5MA$  at ramp-down
- Scenario S3:  $I_{pl} = 17MA$  at flat-top,  $V_{loop} = 0.0V$  for  $I_{pl} = 13 \rightarrow 5MA$  at ramp-down

Simulation results are shown in Figs.6-7. It seems to be advantageous to operate at the maximum flat-top current for which a safe and stable operation can be assured, as not only fusion power gets considerably enhanced as expected, but also resistive and sawtooth-induced flux consumption  $\Psi_{res}$  and  $\Psi_{saw}$  do not increase substantially in the flat-top phase. Comparing scenarios with  $I_{pl} = 17MA$  and  $I_{pl} = 15MA$  with similar flux limit assumptions, we conclude that the  $I_{pl}(t)$  evolution in S3 at  $I_{pl} > 15MA$  must be close to the optimum one.

Techniques that help to minimise the rise in  $\Psi_{res}$  and  $\Psi_{saw}$  during the flat-top are particularly important for the optimisation wrt.  $W_{fus}$ . In S1-S3, the decrease in density and the increase in auxiliary heating and current drive (with slightly more core-localised heat deposition) have helped considerably to keep the flux loss rates at a low level in the burning phase ( $\approx 45\%$  compared to S0). In this period, only a moderate reduction in  $n_e$  can be envisaged though that is within a range where fusion performance remains unaffected and adverse side effects such as an increase in heat flux through the separatrix caused by reduced core radiation as well as higher energies carried by the effluent particles can still be handled.

### 3. HYBRID AND STEADY STATE SCENARIOS

#### 3.1 SPECIFICATION, MAIN ASSUMPTIONS AND MODELS.

The Hybrid scenario is a scenario at intermediate plasma current  $I_p \approx 12\text{MA}$ . The goal is to find out if a long duration discharge can be obtained with the ITER baseline heating mix at an intermediate current value, while the confinement is assumed to be improved with respect to the usual H-mode confinement ( $H_{98(y,2)} = 1.3$ ), as is achieved in many present day experiments. A key element of Hybrid scenario optimisation is to delay as much as possible the occurrence of the  $q = 1$  surface, which is achieved by optimizing both the current ramp-up phase and the current drive scheme during the burn phase. A key novelty of our approach is to use a peaked density profile, in line with state-of-the-art physical understanding of electron transport. This has a beneficial impact on the bootstrap current and makes it easier to sustain  $q$  above unity.

There are two possible options to explore the feasibility of the Steady State (SS) scenario. The first one relies on the assumption of globally improved confinement, without employing a formation of Internal Transport Barrier (ITB). Its design is quite similar to the Hybrid scenario but at reduced plasma current  $I_p = 10\text{MA}$ . At this current, assuming improved confinement with  $H_{98(y,2)} = 1.4$  and making use of the maximum power available in the baseline ITER heating mix plus adding 15MW of LHCD, allows reaching fully non-inductive current drive and steady-state conditions. The second option relies on the creation and sustainment of an ITB due to negative magnetic shear as a source of improved confinement. The approach and the transport model used are similar to the ones described in [17], although the scenario has been redeveloped to take into account a peaked density profile.

The following modelling methodology was used for both Hybrid and SS scenarios. First, the scenario is simulated using CRONOS, optimizing the plasma current waveform and the heating & current drive schemes in order to meet the scenario specifications given by IO. The compatibility of the obtained scenario with the PF systems is then assessed using DINACH/CRONOS coupling. First, the “Prescribed CRONOS” mode is run, in which DINA-CH solves the current diffusion and free boundary equilibrium evolution using CRONOS results for kinetic profiles. Finally, the “Self-consistent” mode is run, where DINA-CH and CRONOS are run in coupled mode, resulting in a self consistent evolution of the free boundary equilibrium, current and kinetic profiles, which are evaluated and exchanged between codes on every time step (5ms). The MHD stability of the established scenarios is then checked a posteriori with the MISHKA code.

The plasma control approach differed from the JINTRAC approach by relying on stronger feedback control and very approximate PF coil current programming. Use of the internal VS3 coils was weak. The power supplies were modelled to protect against exceeding the current limits. In both scenarios, the simulations were carried out from an inboard diverted plasma of 0.4MA and finished with a limited plasma with less than 1.0MA. The SS scenario was simulated in the self-consistent mode to the full 3000 seconds.

### 3.2 THE MAIN MODELLING RESULTS.

#### *Hybrid scenario*

The baseline heating and current drive mix has been optimized to delay as much as possible the occurrence of the  $q = 1$  profile, assuming purely neoclassical resistive current diffusion. Under the modelling assumptions used (essentially, prescribing a peaked density profile and predicting current and temperatures using a transport model yielding an H-mode energy confinement enhancement factor of  $H_{98(y,2)} = 1.3$ ) a scenario where the safety factor  $q$  remains above unity during 1000s burn has been obtained at  $I_p = 12\text{MA}$  ( $q_{95} = 4.3$ ). This scenario uses the ITER baseline heating mix with maximum power during the burn phase: 20MW ICRH, 33MW NBI and 20MW ECCD (@  $\rho = 0.4$ ). In addition, the optimised pre-heating requires the following: i) apply 8MW ECCD early heating after X-point transition, ii) start main heating at  $I_p = 10\text{MA}$  during ramp and iii)  $dI_p/dt = 0.18\text{MA/s}$ . A fusion gain of  $Q = 8$  is thus sustained during 1000 s of burn. Simulations have been also carried out to study the sensitivity of chosen scenario to variations of plasma shape, density peaking,  $H_{98(y,2)}$  factor, pedestal temperature, amount of pre-heating during the current ramp-up. The case of an abrupt, artificially imposed, H to L back transition has also been examined. The main characteristics of the optimised Hybrid scenario are shown on Figure 8.

The coupled DINA-CH/CRONOS simulations showed that small differences between the equilibriums simulated by the combined codes and CRONOS on its own could lead to drifting of the  $q$ -profile during these long pulses especially the appearance of a current hole on axis. This was rectified by modifying the heating and current drive waveforms, but the result shows that control of the  $q$ -profile is necessary for these long pulses. Since the Hybrid scenario uses a lower level of plasma current and energy, fast transient phenomenon, such as H-L transition, do not push the control system beyond its limit. Our control scheme was sufficient to prevent the plasma from being limited outboard or inboard during the fast transient although early HL transitions at EOF might lead to transient wall contact.

#### *Results for the Steady State scenario without ITB.*

This scenario relies on the assumption of globally improved confinement. Its design is quite similar to the hybrid scenario presented above, at reduced plasma current  $I_p = 10\text{MA}$ . At this current, assuming improved confinement with  $H_{98(y,2)} = 1.4$  and using the maximum power available in the baseline ITER heating mix plus adding 15MW of LHCD allows reaching fully non-inductive current drive and steady-state conditions. Density peaking factor  $n_e(0)/\langle n_e \rangle = 1.5$  is assumed, which increases bootstrap current and LHCD efficiency (lower edge density). 3000s of plasma burn have been simulated showing that steady-state conditions are reached (see Figure 9). A fusion gain  $Q$  close to 5 is obtained.

#### *Results for the Steady State scenario with ITB.*

This scenario relies on the assumption of improved confinement via the creation and sustainment

of an ITB due to negative magnetic shear. The scenario uses  $I_p = 8\text{MA}$  with a pure RF heating & current drive scheme (20MW ECCD, 20MW ICRH) tailored to sustain the ITB via a proper current alignment. NBCD is not used because it would drive current inside mid-radius and prevent the ITB sustainment. Instead, 20MW of LHCD are added with respect to the ITER baseline heating mix to drive non-inductive beyond mid-radius. As in the Hybrid scenario, the q-profile drifted. A simple controller was tested to maintain an appropriate core current density. During the 3000 second pulse, a single change to the current drive brought the average loop voltage down to 0.003 Volt. Although q-profile control is needed, a very simple implementation was adequate.

## CONCLUSIONS

All reference ITER scenarios have been self-consistently simulated using coupling between 1.5D transport and 2D free boundary evolution equilibrium codes. New Hybrid and Steady- State scenarios with peaked density profiles have been developed, including current ramp-up and ramp-down, and could be controlled within the limits of the ITER PF systems. Simulation of all baseline scenarios finds compatibility with the present PCS design. Sensitivity study show that optimisation of all baseline scenarios is possible. Further work is needed to complete this study. Studies of L-H and H-L transitions suggest PCS can control plasma, but near or outside limits for some H-L cases. Further work on shape and position control is required.

## ACKNOWLEDGEMENTS

This work was partly funded by the ITER Organisation and F4E under grant G255. The views and opinions expressed herein do not necessarily reflect those of the F4E or those of the ITER Organization.

## REFERENCES

- [1]. Wiesen S. et al., JINTRAC-JET modelling suite, JET ITC-Report 2008.
- [2]. Albanese R., Mattei M., Calabrò G., Villone F., ISEM 2003, Versailles, France.
- [3]. Artaud J.F. et al., Nuclear Fusion **50**, 043001 (2010).
- [4]. Kim S.H. et al., Plasma Physics and Controlled Fusion **51**, 105007 (2009).
- [5]. Erba M. et al, 1997 Plasma Physics and Controlled Fusion **39** 261.
- [6]. Parail V. et al. 2009 Nuclear Fusion **49** (2009) 075030.
- [7]. Imbeaux F. et al. 2011 Nuclear Fusion **51** (2011) 083026.
- [8]. Waltz R.E. 1997 Physics of Plasmas **4** 2482.
- [9]. Martin Y. R. et al. Journal of Physics: Conference Series **123** (2008) 012033
- [10]. Snyder P.B. et al Nuclear Fusion **51** (2011)103016
- [11]. Houlberg W.A., Nuclear Fusion **27** (1987) 1009.
- [12]. Mantica P. et al., Proc. 23rd IAEA Fusion Energy Conference (Daejon, Rep. of Korea)
- [13]. Citrin J. et al. "Predictive transport analysis of JET and AUG hybrid scenarios", EPS 2011.

- [14]. Citrin J. et al. Nuclear Fusion **50** (2010) 115007.  
 [15]. Nunes I.M. et al., “ITER similarity current ramp-down experiments at JET”, EPS 2011.  
 [16]. Chapman I.T. et al., “Sawtooth control in tokamak plasmas”, EPS conference, 2011.  
 [17]. J. Garcia et al, Plasma Physics and Controlled Fusion **50** (2008) 124032  
 [18]. S.H. Kim, J.F. Artaud et al, Plasma Physics and Controlled Fusion **51** (2009) 105007

Plasma major radius $R_0$	$\approx 6.2\text{m}$
Plasma minor radius $a_0$	$\approx 2.0\text{m}$
Toroidal field strength at $R_0$	$\approx 5.3\text{T}$
Plasma fuel	1:1 D–T mixture
Flat-top plasma current	$\approx 15\text{MA}$
Flat-top Greenwald fraction	$\approx 80\text{-}85\%$
$\alpha_C$	$\approx 1.7\text{-}1.9$
ETB width on outer mid-plane	$\approx 6\text{-}8\text{cm}$

*Table 1: OD parameters for the Case #001 scenario.*

<b>Time (s)</b>	<b>ECRH/ICRH/NBI (MW)</b>	<b><math>I_{PL}</math> (MA)</b>	<b>Confinement state</b>
1.3–20	0/0/0	0.5–5.4	L–mode
20–80	<20/0/0	5.4–15	L–mode
80–120	0/20/33	15	H–mode
120–530	0/7/33	15	H–mode
530–630	0/20/33	15–7.5	L–mode
630–650	10/10/0	7.5–6.0	L–mode
650–700	10/0/0	6.0–2.2	L–mode
700–723	0/0/0	2.2–0.5	L–mode

*Table 2: Heating scheme, plasma current and confinement state for the Case #001 scenario.*

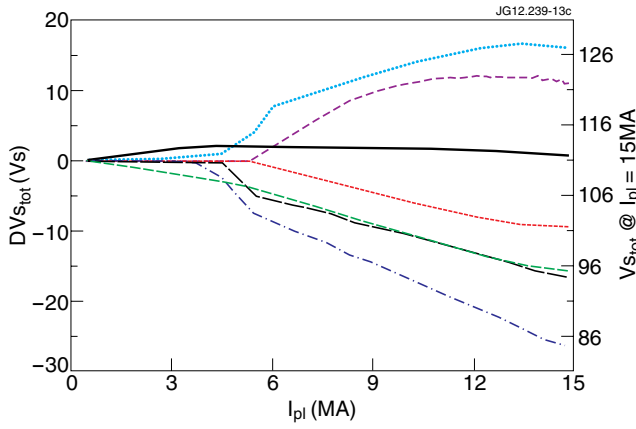


Figure 1: Deviation in total  $V_s$  consumption during current ramp-up with respect to the reference case, for 20% of  $n_{GW}$  (green), 0 MW (magenta) and 20 MW (red) of ECRH, 30 eV of initial boundary temperature (black, reference case: 100 eV), -30% (cyan), +30% (blue dashed) and +66% of  $dI_{pl}/dt$  (blue solid).

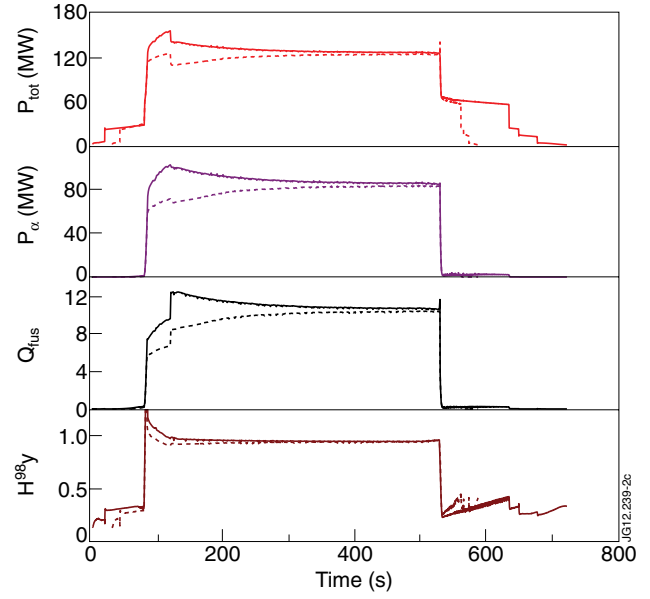


Figure 2: Total deposited heating power, alpha heat deposition, fusion  $Q$  and  $H_{98y}$  (from top to bottom) for the complete reference scenario (solid) and the maximum ramp-rate scenario (dashed).

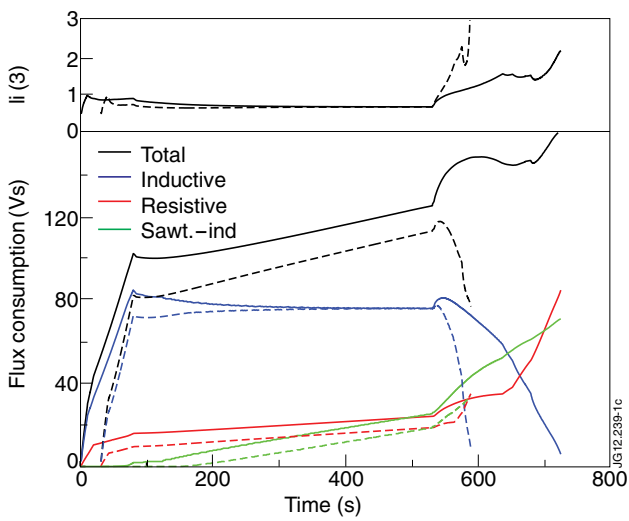


Figure 3:  $I_l(3)$ , total, inductive, resistive and sawtooth-induced  $V_s$  consumption (from top to bottom) for the complete reference scenario (solid) and the maximum ramp-rate scenario (dashed).

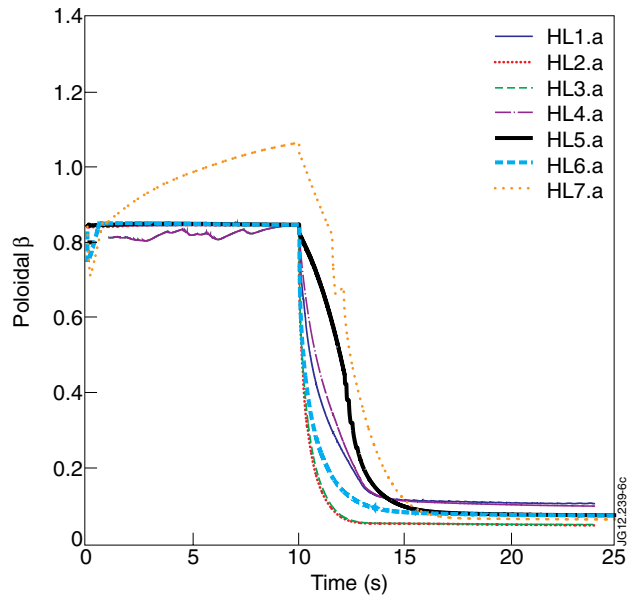


Figure 4:  $\beta_{pol}$  evolution for seven extreme cases with H-L transition.

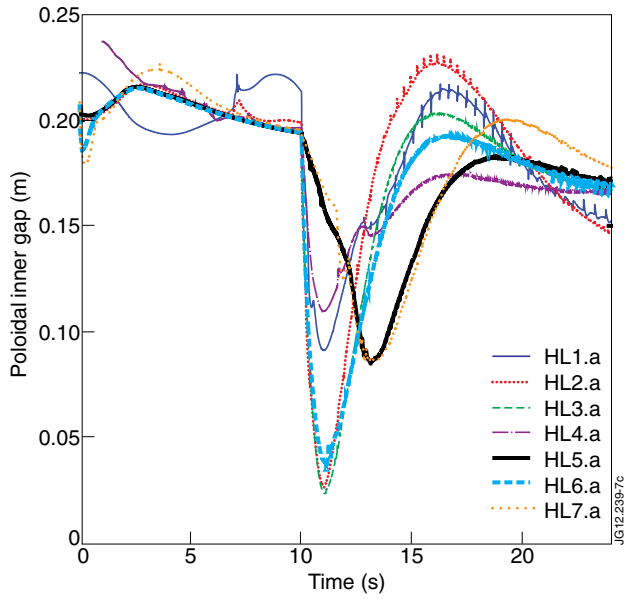


Figure 5: Time histories of inner gaps for seven extreme cases

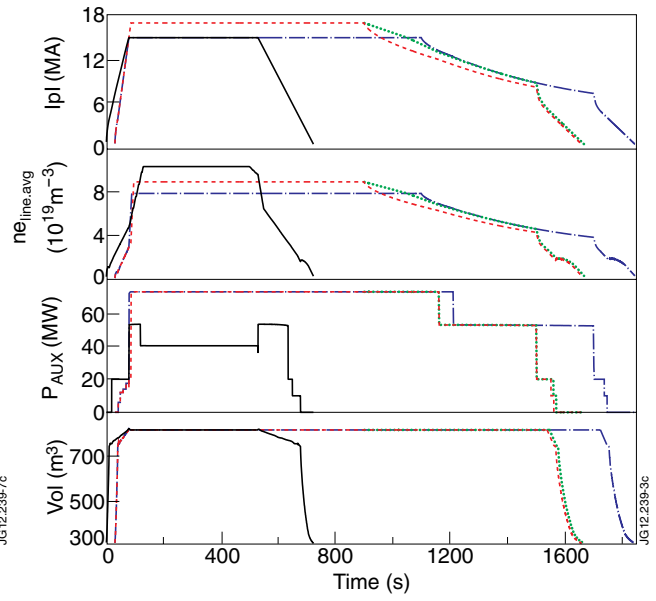


Figure 6: Plasma current  $I_{pl}$ , Thermal energy  $W^{th}$ ,  $P^{fus}$ ,  $Q_{fus}$  and  $H98(y,2)$  for S0 (black), S1 (blue), S2 (red), S3 (green).

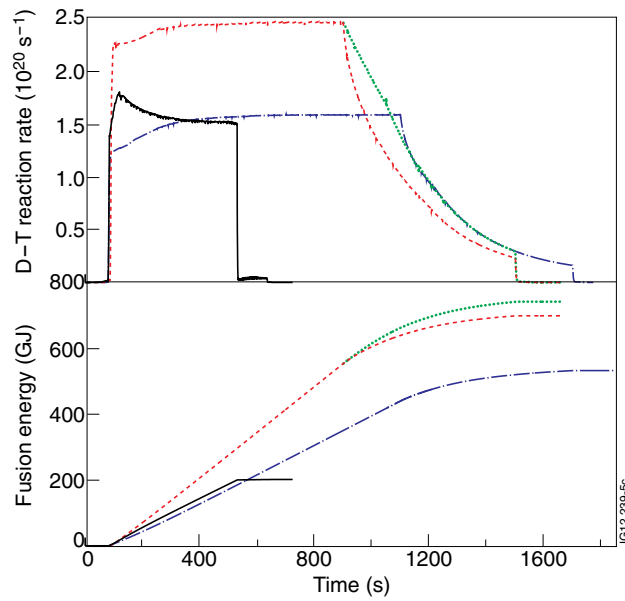


Figure 7: Fusion reaction rate (top) and  $W_{fus}$ (bottom), for S0 (black), S1 (blue), S2 (red) and S3 (green).

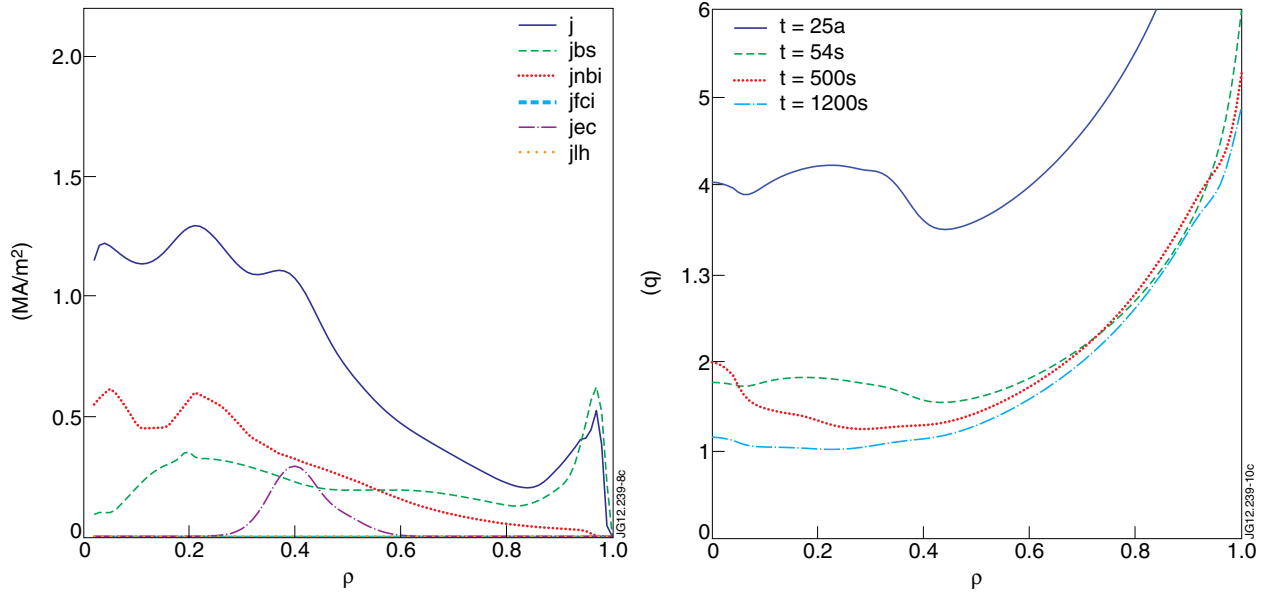


Figure 8: Left: Current density profiles at the end of the burn phase of ITER hybrid scenario ( $t = 1200s$ ). bootstrap (green), fast wave (red), Lower Hybrid waves (yellow), Electron Cyclotron current drive (purple), total (blue). Right: Evolution of the safety factor profile for the hybrid scenario.

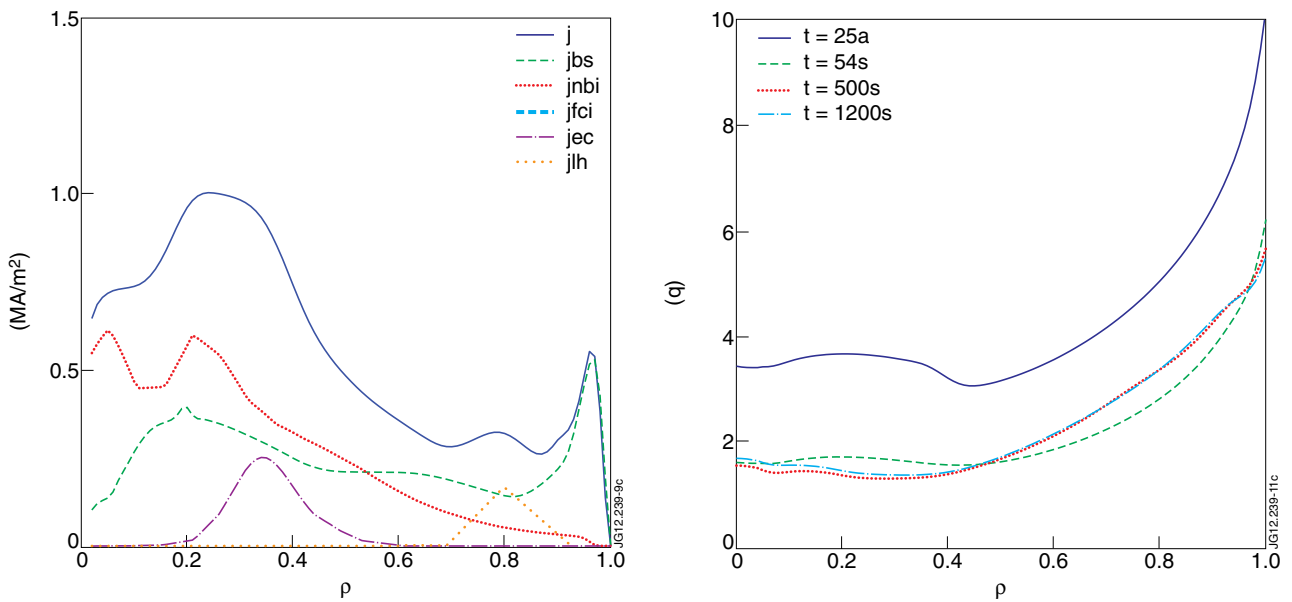


Figure 9: Left: Current density profiles during the SS the burn phase of ITER steady-state scenario without ITB. bootstrap (green), fast wave (red), Lower Hybrid waves (yellow), Electron Cyclotron current drive (purple), total (blue). Right: Evolution of the safety factor profile for the SS scenario without ITB.